Article

Adsorption states of typical intermediates on Ag/Al₂O₃ catalyst employed in the selective catalytic reduction of NO$_x$ by ethanol

Hua Deng, Yunbo Yu *, Hong He #

State Key Joint Laboratory of Environment Simulation and Pollution Control, Research Center for Eco-Environmental Sciences, Chinese Academy of Sciences, Beijing 100085, China

ABSTRACT

The adsorption of ethanol and important intermediates onto Ag/Al₂O₃ catalyst employed in the selective catalytic reduction of NO$_x$ by ethanol was simulated by density functional theory. Considering the interaction between Ag metal and Al₂O₃ support, typical Ag–O–Al entities, i.e., Ag–O–Al$_{tetra}$ and Ag–O–Al$_{octa}$, (tetra = tetrahedral and octa = octahedral refer to the coordination sites of Al), were selected as potential adsorption sites on the surface of the catalyst. Ethanol, and enolic and isocyanate species were preferentially adsorbed and activated by Ag–O–Al$_{tetra}$ entities rather than by Ag–O–Al$_{octa}$ entities. The strong Lewis acidity of Al$_{tetra}$ in the Ag–O–Al$_{tetra}$ entity was very important, enabling the entity to accept an electron via forward donation from either the C–O σ bond in ethanol or the N–C σ bond in the –NCO species. Moreover, the hybridization of the Ag and Al orbitals was critical for electron back donation from the Ag–O–Al$_{tetra}$ entity to the C–C π bond in the enolic species or N–C π bond in the –NCO species. The significant activation of the N–C bond in –NCO on the Ag–O–Al$_{tetra}$ sites facilitated cleavage of –NCO to form N₂. Thus, we can conclude that the acidity of the Al site and the interaction between Ag and Al play key roles in the selective catalytic reduction of NO$_x$ by ethanol over Ag/Al₂O₃.

1. Introduction

Nitrogen oxides (NO$_x$) are mainly produced by the combustion of fuels from mobile and stationary sources, which leads to serious air pollution in the form of acid rain, photochemical smog, and haze [1,2]. Currently, the removal of NO$_x$ from lean-burn exhausts remains a major challenge in environmental catalysis because, in the presence of excess oxygen, NO$_x$ cannot be efficiently removed by traditional three-way catalysts. Among the developed technologies to eliminate NO$_x$ emission from lean-burn exhausts, the selective catalytic re-duction of NO$_x$ by hydrocarbons (HC-SCR) is a potential method, which has attracted much attention in the past few decades [3–7]. Al₂O₃-supported Ag catalyst Ag/Al₂O₃ is considered as one of the most effective materials for the HC-SCR process in the presence of excess oxygen [8–10]. And ethanol as HC is extremely effective for the SCR of NO$_x$ [11]. Thus, establishing a relationship between the structural features of Ag/Al₂O₃ catalysts and their catalytic activity toward ethanol-SCR is crucial for designing a highly efficient HC-SCR system.

As generally accepted, to ensure high activity of Ag/Al₂O₃ in HC-SCR, Ag (the active component) must interact strongly with

the Al_2O_3 support. By comparing the kinetics features of as-prepared Ag/Al_2O_3 and samples leached by dilute nitric acid, She et al. [12] confirmed that Ag species, particularly Ag^+ cations, strongly bind to the Al_2O_3 support, possibly as Ag–O–Al entities. Such entities were demonstrated as the active sites in SCR of NO_x by CH_4. In another study, Zhang et al. [13] examined the activity of different Ag/Al_2O_3 catalysts prepared from different Al precursors in the NO_x reduction by C_3H_6. The authors showed that the best SCR activity could be achieved in the presence of Ag catalysts employing AlOOH as the precursor because of the generation of heavily populated Ag–O–Al entities. Based on theoretical simulations of the local structure of Ag species and their interface with γ-Al_2O_3 (110) surface [14], more recently, we found that orbital mixing among Ag, O, and Al in Ag/γ-Al_2O_3 plays a key role in the reduction of NO_x by ethanol. However, more accurate atomic description of the interface between the Ag species and different planes of the Al_2O_3 surface remains challenging. Liu et al. [15] and Hu et al. [16] studied the alumina system based on first-principles methods. The studies showed that different exposed surfaces of alumina exhibited different abilities in anchoring active components such as Pd clusters and adsorbing NO_x [15,16]. γ-Al_2O_3 displays two major exposed surfaces, namely (100) and (110), whereby the Al coordination environments are different. The Al_2O_3 (110) surface corresponds to a rectangular oxygen atom sublattice and exposes valence-unsaturated surface Al atoms such as tetrahedral Al (AlO_4; Al_{tetra}), accounting ~70%–83% of the total surface area [17,18]. In contrast, the Al_2O_3 (100) surface that corresponds to a square oxygen atom lattice is less abundant and accounts for 17% of the surface area. It exposes valence-saturated pentahedral Al (AlO_5; Al_{pen}) and/or octahedral Al (AlO_6; Al_{octa}) coordination sites [17,18]. The coordination of Al atoms on the alumina surface is of particular importance because the valence-unsaturated surface Al atoms are a source of surface Lewis acidity. To some extent, the coordination of Al atoms on the surface is the key to the catalytic process. However, the relationship between the location of Ag species and the corresponding activity is poorly understood.

The mechanisms of NO_x reduction by hydrocarbons have been extensively explored [3–6,19–21]; the general reaction pathway is shown in Scheme 1. First, NO is oxidized to NO_2 by O_2, which results in the formation of surface nitrates. Second, a HC reductant, such as ethanol or propene, is partially oxidized to acetate and enolic or other oxygenated species. Finally, the oxygenated species preferentially react with the nitrates to produce N_2 and CO_2 via the formation and reaction of –NCO and/or –CN species. Two typical processes should be addressed in this mechanism: (1) the partial oxidation step of hydrocarbons and (2) the surface reaction between nitrates and oxygenates. Among the oxygenated species possible, a novel surface enolic species has been suggested as an important intermediate that is related to the high efficiency observed for the SCR of NO_x by alcohols [11,22–24]. Considering Al_2O_3-based catalysts, the rate-determining step for HC-SCR is thought to be the surface reaction between nitrates and oxygenates [3,20,25], during which the product –NCO species is considered as the most important intermediate [26–28].
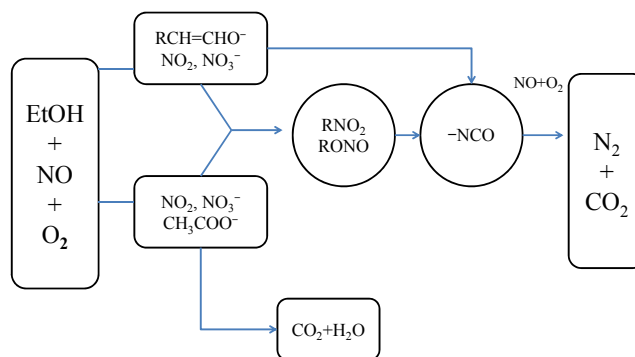
Scheme 1. Reaction mechanism of SCR of NO_x over alumina-based catalysts.

Density functional theory (DFT) calculations have been increasingly employed to predict the interactions between adsorbates and catalytic sites. Such DFT methods provide accurate geometries, and reasonable energetics for molecules adsorbed onto particular surfaces are sufficient to determine the active sites. For instance, in previous studies, we identified the structure of the enolic species and the associated infrared spectrum, which were confirmed by comparison of the DFT calculations and experimental findings [22–24]. The presence of –NCO species has also been simulated on Ag clusters using DFT calculations for correlation with the experimentally determined infrared features of –NCO [29,30]. However, reports on the detailed geometry and electronic structures of the chemical bonds of enolic and isocyanate species interacting with Ag–O–Al entities on the Ag/Al_2O_3 surface are scarce.

In this study, the adsorption of predominant Ag^+ species onto Al_2O_3 (110) and (100) surfaces (Al_{tetra} and Al_{octa} sites, respectively) forming Ag–O–Al_{tetra} and Ag–O–Al_{oct} entities, respectively, was modeled by DFT methods. Adsorbates, CH_3CH_2OH, $CH_2=CHO^-$, and –NCO species, on both entities were simulated and compared. As observed, the adsorption and activation of CH_3CH_2OH, $CH_2=CHO^-$, and –NCO species proceeded preferentially on the Ag–O–Al_{tetra} entities rather than on the Ag–O–Al_{octa} entities. The strong Lewis acidity of the Al_{tetra} site and interaction between Ag and Al are believed to play key roles in such a phenomenon.

2. Methods

The crystallographic data of the γ-Al_2O_3 bulk structure was obtained from the model reported by Digne et al. [17,18]. The structure was geometrically optimized further to explore the HC-SCR process. The calculated lattice parameters of bulk Al_2O_3 are a = 5.587 Å, b = 8.413 Å, c = 8.068 Å, and $β$ = 90.59°, in good agreement with previous calculations [17,18]. The dehydrated (100) and (110) surfaces of γ-Al_2O_3 were modeled as (2×2) supercells and four-layered thick slabs, containing 200 and 160 atoms, respectively (lattice parameters of (100) and (110) surfaces: a = 11.174 Å, b = 16.826 Å and a = 16.826 Å, b = 16.136 Å, respectively).

The periodic DFT geometry calculations were performed using a plane-wave method as implemented in the Materials

Studio Modeling program CASTEP. The exchange-correlation functional was treated within the generalized gradient approximation parameterized by Perdew and Wang PW91. The electron–ion interaction was described by the ultrasoft potential in reciprocal space. The inter-slab distance was maintained at 20 Å to avoid inter-slab interactions in the periodic systems. A tight convergence of the plane-wave expansion was obtained with a kinetics energy cut-off of 400 eV. According to our earlier convergence test, the k-point sets of (2×1×1) and (1×1×1) were used for the Al_2O_3 (100) and Al_2O_3 (110) surfaces, respectively, as consistent with other reports [15,16]. The bottom two layers were fixed to the positions of the relaxed alumina slab, whereas the other atomic layers together with the adsorbents were fully relaxed. Spin polarization was considered in all calculations. The electronic density differences and Mulliken charge were calculated at the same level of theory.

The adsorption energies of the AgO unit and adsorbates (C_2H_5OH, $CH_2=CHO^-$, $-NCO$) on either the Al_2O_3 surface or the Ag/Al_2O_3 surface were calculated as follows

$$E_{ad} = E_{adsorbate+surface} - (E_{surface} + E_{adsorbate}),$$

where $E_{adsorbate+surface}$ and $E_{surface}$ are the total energies of the adsorbed system and alumina slab with or without AgO unit, respectively; and E_{ad} reflects the stability of the adsorbates on either the Al_2O_3 or the Ag/Al_2O_3 surface. Negative E_{ad} values indicate that the adsorbed state is energetically favorable. Additionally, bond overlap population (BOP) calculations were performed on the periodic systems. Positive BOP values indicate that a bond is formed, whereas negative BOP values indicate non-bonding [16]. The electronic structures were analyzed in terms of density of states (DOS) and partial density of states (PDOS).

3. Results and discussion

3.1. Ag–O–Al entities on Ag/Al₂O₃

Ag/Al_2O_3 has been studied as a promising catalyst owing to its high activity in SCR of NO_x by hydrocarbons in the presence of excess oxygen. The silver species play the most important role in the HC-SCR process. As widely accepted, different types of Ag species, such as isolated Ag^+ cations, oxidized silver clusters ($Ag_n^{\delta+}$), and metallic silver clusters (Ag_n^0), are present on the Ag/Al_2O_3 catalysts before and during the HC-SCR process [31–35]. Among the different species, oxidized silver (Ag^+ and/or $Ag_n^{\delta+}$) is believed to be the active species for NO_x reduction by hydrocarbons [12,31–35]. The optimum silver loading is typically ~2–4 wt%, at which the formation of a Ag–O layer is predominant on the Al_2O_3 surface [10,11,14,22,24]. Other studies [12,31,36] also suggested that the presence of Ag^+ species is predominant and should be considered as the active species for the reduction of NO_x. In this study, different types of Al sites that bond with oxidized Ag were considered.

There are 16 Al atoms on the 2×2 (110) surface. According to the coordination environment, in Fig. 1(a), three types of Al atoms could be identified i.e., Al_{trip} (AlO_3, originating from bulk Al_{tetra}), and $Al_{tetra-a}$ and $Al_{tetra-b}$ (AlO_4, originating from bulk Al_{octa}). As observed in Fig. 1(b), the stable structure of the (100)
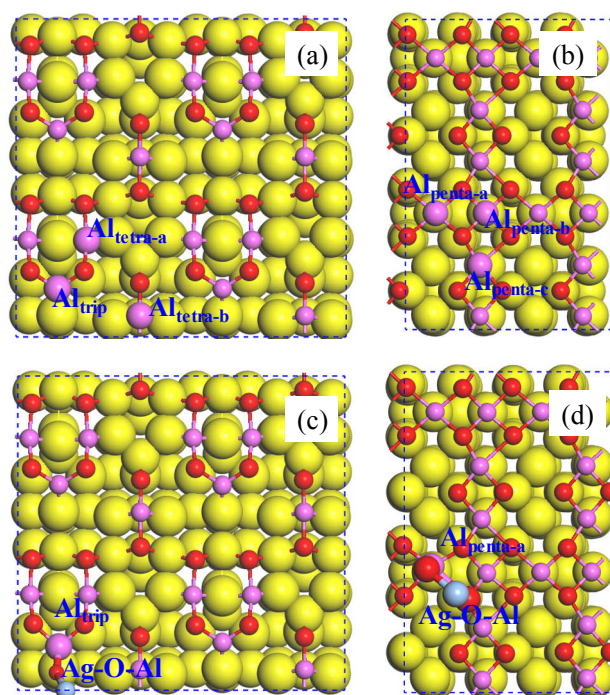

Fig. 1. Optimized periodic models of Al_2O_3 and Ag/Al_2O_3 catalysts. (a) Al_2O_3 (110) surface; (b) Al_2O_3 (100) surface; (c) Ag/Al_2O_3 with Ag–O–Al_{tetra} entities; and (d) Ag/Al_2O_3 with Ag–O–Al_{octa} entities.

surface exhibits penta-coordinated Al atoms (Al_{penta}; AlO_5, derived from bulk Al_{octa}). Likewise, there are 16 Al atoms on the 2×2 (100) surface, and three types of Al atoms can be observed (denoted as $Al_{penta-a}$, $Al_{penta-b}$, $Al_{penta-c}$). Accordingly, the AgO unit can be anchored to these two types of surfaces via six types of interactions.

Thus, Al_{trip}, $Al_{tetra-a}$, and $Al_{tetra-b}$ derived from the 2×2 (110) surface, and $Al_{penta-a}$, $Al_{penta-b}$, and $Al_{penta-c}$ derived from the 2×2 (100) surface were selected as the Ag anchoring sites to construct the Ag/Al_2O_3 models, denoted as Models 1–6, respectively.

Based on the ^{27}Al MAS NMR characterization of the Ag/Al_2O_3 catalyst, two types of stable Al atoms (Al_{tetra} and Al_{octa}) could be observed on the Ag/Al_2O_3 catalyst [37–40]. Ag^+ formed Ag–O–Al_{octa} entities upon interaction with Al_{octa} sites (derived from Al_{penta}) that were the main anchoring sites [37, 39–41]. Furthermore, Al_{tetra} sites were believed to play an important role in stabilizing Ag, whereas Al_{trip} sites on the Al_2O_3 (110) surface seemed to be the precursors for the formation of Ag–O–Al_{tetra} entities. Among the six constructed models, only Model 1 can be considered as a Ag/Al_2O_3 catalyst containing Ag–O–Al_{tetra} entities, whereas Models 4–6 can be considered as Ag/Al_2O_3 catalysts containing Ag–O–Al_{octa} entities. Comparison of the adsorption energies of Models 4–6 revealed that Model 4 (Ag^+ anchored to $Al_{penta-a}$ sites on the Al_2O_3 (100) surface) exhibited the most negative adsorption energy value, thus indicating that Model 4 is the most stable catalyst configuration. Thus, Model 1 (Ag–O–Al_{tetra}) and Model 4 (Ag–O–Al_{octa}) were selected for the subsequent studies.
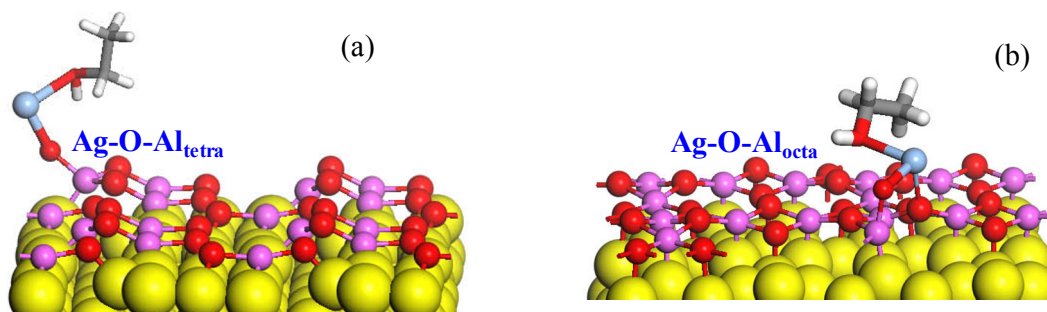
Following Ag loading, the Ag species in the two entities

Fig. 2. Structure of a CH₃CH₂OH molecule adsorbed onto (a) Ag/Al₂O₃ (110) surface (Ag–O–Al$_{tetra}$ entities) and (b) Ag/Al₂O₃ (100) surface (Ag–O–Al$_{octa}$ entities).

Table 1
DFT-calculated adsorption energies, structural parameters, and BOP values.

Free state	Bond	Ag–O–Al$_{tetra}$			Ag–O–Al$_{octa}$			Ref. (free C₂H₅OH, CH₂CHOH, HNCO)	
		E_{ad}	Bond length	BOP	E_{ad}	Bond length	BOP	Bond length	BOP
C₂H₅OH	C–O	−0.43	1.459	0.46	−0.38	1.446	0.48	1.439	0.48
CH₂=CHO⁻	C–O	−1.99	1.312	0.76	−1.95	1.291	0.83	1.375	0.58
	C–C		1.364	1.09		1.383	1.04	1.331	1.23
–NCO	N–C	−3.84	1.236	1.39	−3.49	1.215	1.53	1.227	1.33

(E_{ad}: eV; bond length: Å; and Mulliken charge: e)

maintained the +1 oxidation state, as consistent with our previous studies [14, 31]. The Ag–O bond length in crystalline Ag₂O was 2.04 Å. The average Ag–O bond lengths in Ag–O–Al$_{tetra}$ and Ag–O–Al$_{octa}$ were 2.02 and 2.09 Å, respectively. This finding indicates that when compared with the crystalline Ag₂O, anchoring to the Al₂O₃ (110) surface strengthens the Ag–O bond, whereas anchoring to the Al₂O₃ (100) surface slightly weakens the Ag–O bond.

3.2. Structures of intermediates adsorbed onto Ag–O–Al entities

The HC-SCR of NO$_x$ over Ag/Al₂O₃ catalysts is primarily determined by the surface mechanism. Using C₂H₅OH as a reductant results in significantly higher NO$_x$ conversion when compared with C₃H₆, especially at low reaction temperatures [11]. Generally, the activation of the reductant is considered as the initial and key step in the HC-SCR process [3–6,19–21]. Ag sites are widely accepted as the activation spots for the reductant [22–24]. Thus, the adsorption of molecular C₂H₅OH onto typical types of Ag–O–Al entities was simulated. The results of the geometry optimization of C₂H₅OH in intimate contact with a Ag site are shown in Fig. 2. The O atom in C₂H₅OH is directly linked to a Ag⁺ ion on the surface. The bond features (including bond length and BOP values) and Mulliken charges are summarized in Tables 1 and 2, respectively.

The adsorption energies of ethanol onto Ag–O–Al$_{tetra}$ and Ag–O–Al$_{octa}$ entities were −0.43 and −0.38 eV, respectively. These results indicate that the Ag–O–Al$_{tetra}$ site has a stronger affinity for ethanol than the Ag–O–Al$_{octa}$ entity. Furthermore, the structure of C₂H₅OH and surface did not change considerably except for the elongation of the C–O bond and H–O bond following interaction with both Ag–O–Al entities. The C–O bond in the isolated C₂H₅OH molecule was 1.439 Å. Adsorption of

ethanol onto the Ag–O–Al$_{tetra}$ and Ag–O–Al$_{octa}$ entities resulted in C–O bond length increases to 1.459 and 1.446 Å, respectively. The BOP values resulting from the adsorption of the C–O bond onto the Ag–O–Al$_{tetra}$ and Ag–O–Al$_{octa}$ entities were 0.46 and 0.48, respectively. Taking into account the BOP value of 0.48 in free C₂H₅OH, we could conclude that the presence of Ag⁺ ion on the Al$_{tetra}$ site could perturb the ethanol molecule to a greater extent than that on the Al$_{octa}$ site. On the other side, the H–O bond length in the ethanol molecule was 0.977 Å. The adsorption of ethanol onto the Ag–O–Al$_{tetra}$ and Ag–O–Al$_{octa}$ entities resulted in H–O bond length increases to 0.984 and 0.978 Å, respectively. This result indicates that the Al site is not only of particular importance in anchoring silver species, but also influences the activation of reductants.

Enolic species (CH₂=CHO⁻), which are derived from the partial oxidation of a given reductant such as ethanol in excess oxygen, have been identified as important intermediates in the HC-SCR process. When compared with acetate (CH₃COO⁻) intermediates, enolic species are more active in the production of important intermediates (such as –NCO) and subsequent reduction of NO$_x$ [22–24]. Thus, studying the adsorption of enolic

Table 2
DFT-calculated Mulliken charges for Ag–O–Al entities and the adsorbed intermediates.

Free state	Entity	Adsorbate	Ag	O	Al
	Ag–O–Al$_{tetra}$	—	0.58	−1.00	1.80
	Ag–O–Al$_{octa}$	—	0.56	−0.58	1.62
C₂H₅OH	Ag–O–Al$_{tetra}$	−0.01	0.70	−0.95	1.77
	Ag–O–Al$_{octa}$	−0.05	0.79	−0.82	1.67
CH₂=CHO⁻	Ag–O–Al$_{tetra}$	−0.31	0.82	−0.95	1.80
	Ag–O–Al$_{octa}$	−0.27	0.69	−0.76	1.67
–NCO	Ag–O–Al$_{tetra}$	−0.56	0.76	−0.86	1.76
	Ag–O–Al$_{octa}$	−0.59	0.89	−0.81	1.69
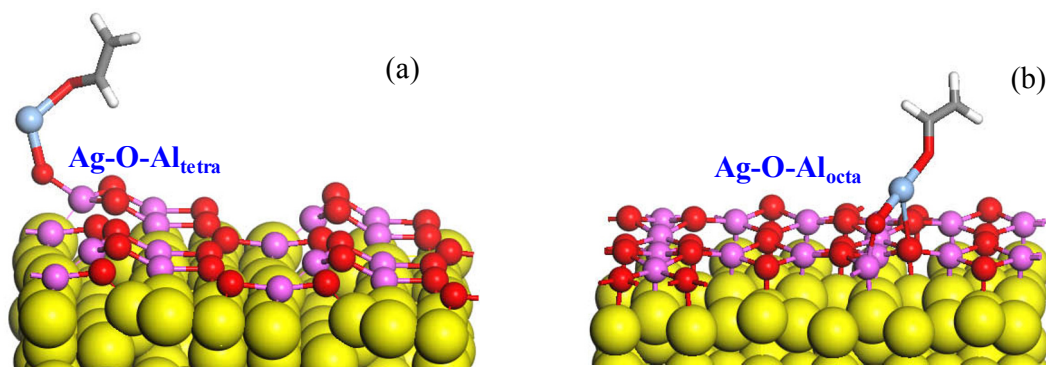
Fig. 3. Structure of CH$_2$=CHO$^-$ adsorbed onto (a) Ag/Al$_2$O$_3$ (110) surface (Ag–O–Al$_{tetra}$ entities) and (b) Ag/Al$_2$O$_3$ (100) surface (Ag–O–Al$_{octa}$ entities).

species onto Ag/Al$_2$O$_3$ catalysts by DFT calculations is important. It is worth noting that that enolic species are in intimate contact with Ag sites [36]. Based on this conclusion, we constructed models of enolic species (CH$_2$=CHO$^-$) interacting with Ag–O–Al$_{tetra}$ and Ag–O–Al$_{octa}$ entities. The optimized models are shown in Fig. 3. The corresponding structure parameters, BOP values, and Mulliken charges are summarized in Tables 1 and 2, respectively.

The adsorption energies of enolic species onto Ag–O–Al$_{tetra}$ and Ag–O–Al$_{octa}$ were −1.99 and −1.95 eV, respectively. This finding indicates that the adsorption of CH$_2$=CHO$^-$ species onto Ag–O–Al$_{tetra}$ entities is preferred over that onto Ag–O–Al$_{octa}$ entities. Following interaction with Ag/Al$_2$O$_3$, the enolic species were mostly unchanged except for the weakening of the C–C bond and strengthening of the C–O bond, which could be deduced by comparison with the structure of free vinyl alcohol. For instance, the C–C and C–O bond lengths in free vinyl alcohol were 1.331 and 1.375 Å, respectively. In contrast, the corresponding C–C bond lengths in the enolic species following adsorption onto Ag–O–Al$_{tetra}$ and Ag–O–Al$_{octa}$ entities increased to 1.364 and 1.383 Å, respectively. And the corresponding C–O bond lengths decreased to 1.312 and 1.291 Å, respectively. To evaluate changes in bond order, BOP values were determined. The BOP values of the C–C and C–O bonds in vinyl alcohol were 1.23 and 0.58, respectively. Following adsorption onto Ag–O–Al$_{tetra}$ and Ag–O–Al$_{octa}$ entities, the BOP values of the C–C bond decreased to 1.09 and 1.04, respectively. And the corresponding BOP values of the C–O bond increased to 0.76 and 0.83, respectively. Owing to the similar bond changes, the two different enolic species are believed to exhibit similar activities.

Accordingly, we can conclude that the Ag–O–Al$_{tetra}$ entity is more suitable as an adsorption site than Ag–O–Al$_{octa}$ based on the lower adsorption energy obtained.

Isocyanate species (−NCO) may form upon thermal decomposition of a precursor complex, NO$_x$C$_y$H$_z$, during the reduction of NO$_x$ by hydrocarbons [11,42]. The activity of −NCO species was proved by many groups [26–28], and its key role in the HC-SCR process was widely confirmed [3–6,19–21]. Studying the configuration of −NCO species adsorbed onto Ag–O–Al entities is very important to understand the activity of −NCO and discern the active sites on the surface of the catalyst.

The adsorption energies of −NCO adsorbed onto Ag–O–Al$_{tetra}$ and Ag–O–Al$_{octa}$ entities were −3.84 and −3.49 eV, respectively. This indicates that the Ag–O–Al$_{tetra}$ entity promotes the adsorption of −NCO to a greater extent than the Ag–O–Al$_{octa}$ entity. After adsorption, a small deformation was observed in the configuration of −NCO. For instance, The N–C and C–O bond lengths in free isocyanic acid were 1.227 and 1.185 Å, respectively. The corresponding N–C bond lengths in −NCO following adsorption onto Ag–O–Al$_{tetra}$ and Ag–O–Al$_{octa}$ entities were 1.236 and 1.215 Å, respectively, whereas the C–O bond lengths increased to 1.196 and 1.203 Å, correspondingly. Based on a former study [43], bond rupture between N and C in −NCO is essential upon reaction with NO$_2$ to produce N$_2$. Thus, considering the activation of the N–C bond is more important than that of the C–O bond in −NCO. In summary, Ag–O–Al$_{tetra}$ sites activated −NCO species to a greater extent than the Ag–O–Al$_{octa}$ entities, as further confirmed by the BOP values. The BOP values of the N–C and C–O bonds in free HNCO were 1.33 and 1.15, respectively. After interacting with Ag–O–Al$_{tetra}$ or Ag–O–Al$_{octa}$

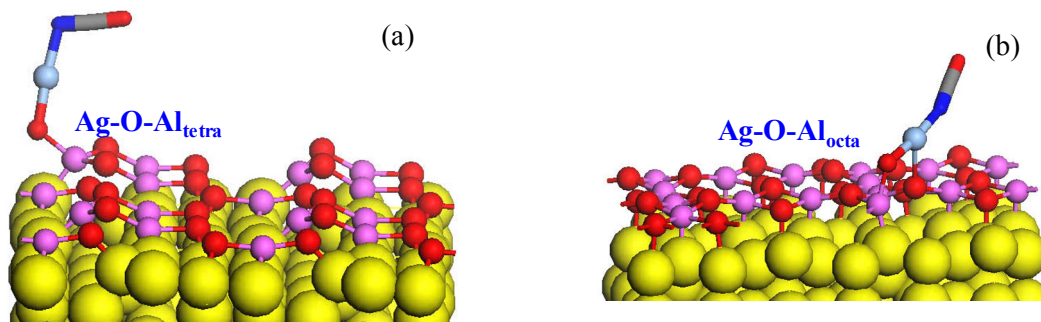**Fig. 4.** Structure of −NCO adsorbed onto (a) Ag/Al$_2$O$_3$ (110) surface (Ag–O–Al$_{tetra}$ entities) and (b) Ag/Al$_2$O$_3$ (100) surface (Ag–O–Al$_{octa}$ entities).

entities, the BOP values of the N–C bond were 1.39 and 1.53, respectively. In contrast, the BOP values of C–O decreased slightly to 1.10 and 1.08, correspondingly. This result indicates that the Ag–O–Al$_{octa}$ entity significantly strengthens the N–C bond so that the –NCO species are stabilized on this site. During the deformation of adsorbates on the Ag/Al$_2$O$_3$ surfaces, discerning orbitals belonging to adsorbates and/or metal involved in the interaction process is of great interest. Thus, the decomposition of orbital method was used to establish the bonding in the three adsorption processes related to CH$_3$CH$_2$OH, CH$_2$=CHO$^-$, and –NCO species.

3.3. Electronic structures of adsorbed intermediates onto Ag/Al$_2$O$_3$ surface

Evaluating DOS is a powerful tool to analyze the energetic levels of slabs. The electronic structures of Ag/Al$_2$O$_3$ and the different adsorbates, C$_2$H$_5$OH, CH$_2$=CHO$^-$, and –NCO, on the catalysts were analyzed to determine the chemical bonding interactions between the metal and adsorbates. The activation of ethanol in the HC-SCR process is considered as the critical step in improving NO$_x$ reduction efficiency. Based on the geometry structure analysis above, we claimed that the presence of Ag–O–Al$_{tetra}$ entities rather than the Ag–O–Al$_{octa}$ entities could significantly activate the C$_2$H$_5$OH molecule by elongating the C–O bond. To understand the changes in the spatial locations of electrons during the adsorption process, the DOS of the catalyst model before and after C$_2$H$_5$OH adsorption was examined, as shown in Fig. 5.

The two C atoms and one O atom in C$_2$H$_5$OH are sp^3-hybridized. All bonds are formed upon overlapping with these sp^3 hybrid orbitals. Thus, the C–H, O–H, C–C, and C–O bonds are all σ bonds. As observed in Fig. 5, the peak around −20 to −18 eV in the free C$_2$H$_5$OH molecule could be ascribed to the C–O σ bond (s bond). After adsorption onto the Ag–O–Al$_{tetra}$ and/or Ag–O–Al$_{octa}$ entities, the energy of the respective σ bonds decreased. However, the σ bond was delocalized on the Ag–O–Al$_{tetra}$ entities and remained localized on the Ag–O–Al$_{octa}$ entities. The electrons from the σ bond in C–O bond displayed a "resonance" with the Ag/Al$_2$O$_3$ catalyst, especially with Al$_{tetra}$ atoms, in the energy range from −21 to −18 eV, as shown in Fig.

5(a), thereby resulting in σ bond forward donation to the catalyst surface. The forward donation from the σ bond to some appropriate hybrid on a partner metal fragment is a classic mechanism, as exemplified by the CO 5σ bond forward donation to the Ni (100) or Pt (111) system [44,45]. By comparing the two Ag–O–Al entities, we could deduce that Al$_{tetra}$ atoms were more prone to accept electrons than Al$_{octa}$ owing to the strong Lewis acidity of Al$_{tetra}$ atoms. Thus, we can conclude that Lewis acidity is a decisive factor that determines the activation of C$_2$H$_5$OH in the HC-SCR process. Table 2 lists the Mulliken charges of Ag, O, Al, and adsorbates. The Mulliken charge of the Al atom in the free Ag–O–Al$_{tetra}$ entity was 1.8 e. Following adsorption, a lower charge of 1.76 e was obtained. This finding confirmed that Al$_{tetra}$ is a Lewis acid site, which can accept electrons from adsorbates. In contrast, the Al atom in Ag–O–Al$_{octa}$ cannot accept electrons from adsorbates, as shown in Table 2.

Enolic species, such as CH$_2$=CHO$^-$, are more active than acetate species, CH$_3$COO$^-$, for interaction with adsorbed NO$_x$. Examining the adsorbed states of enolic species is very important. Fig. 6 displays the electronic structures of CH$_2$=CHO$^-$ adsorbed onto Ag–O–Al$_{tetra}$ and Ag–O–Al$_{octa}$ entities. The free enolate anion exhibits nine valence molecular orbitals, which can be correlated to the nine peaks observed in the DOS diagrams. The peak around −20.5 to −18.5 eV could be ascribed to the C–O σ bond and the peak around −4 to −3 eV could be assigned to the C–C π bond (p bond). After adsorption onto the Ag/Al$_2$O$_3$ catalyst, the energy level of the C–O σ bond decreased. However, the C–O σ bond close to a Ag–O–Al$_{tetra}$ site displayed a "resonance" with the oxide metal surface and was delocalized via electron forward donation. The C–O bond on Ag–O–Al$_{octa}$ did not display any particular "resonances" with the surface of the catalyst and remained localized. Consequently, the C–O bond was strengthened on the Ag–O–Al$_{octa}$ entity. In both cases, the C–C π bonds were delocalized, as shown in Fig. 6. Additionally, the former structure suggested that the C–C bonds were elongated. Back donation, as the interaction mechanism, involving the Ag d orbital and Al p orbital at around −4 to −2 eV to the π bond of C–C, is highly plausible. Consequently, the C–C bond in the enolic species was activated likely due to major influences of the Al support and silver metal.

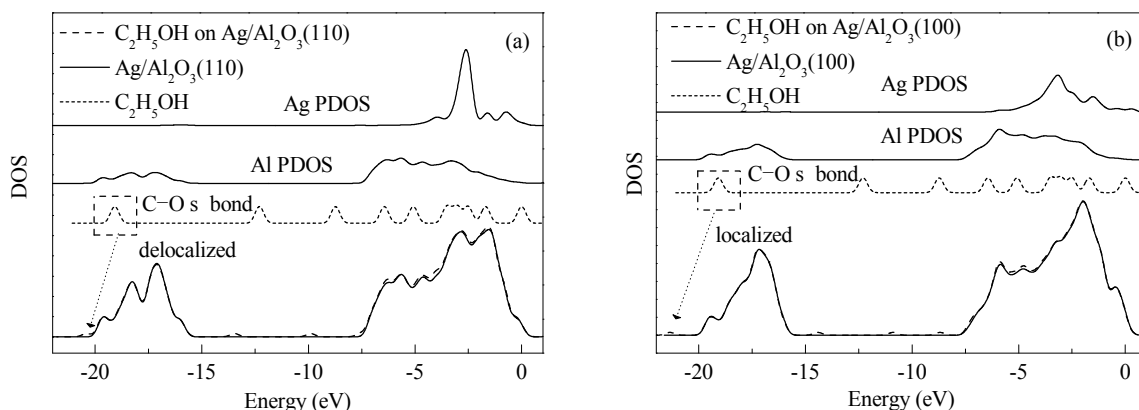Key intermediate –NCO species can directly reduce NO$_x$ to

Fig. 5. Total DOS and atom-resolved projected DOS (PDOS) analysis of CH$_3$CH$_2$OH adsorbed onto (a) Ag/Al$_2$O$_3$ (110) surface (Ag–O–Al$_{tetra}$ entities) and (b) Ag/Al$_2$O$_3$ (100) surface (Ag–O–Al$_{octa}$ entities).

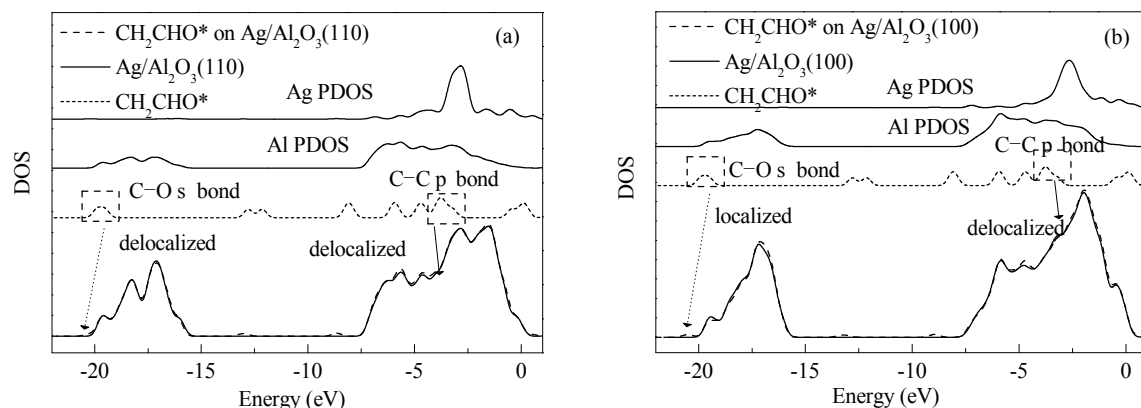**Fig. 6.** Total DOS and atom-resolved projected DOS (PDOS) analysis of $CH_2=CHO^-$ adsorbed onto (a) Ag/Al_2O_3 (110) surface (Ag–O–Al_{tetra} entities) and (b) Ag/Al_2O_3 (100) surface (Ag–O–Al_{octa} entities).

form N_2 and CO_2 or CO. Comparison of the electronic states of –NCO on the two types of Ag–O–Al entities revealed the true active site involved in the reduction of NO_x. Based on the earlier geometry structural analysis, we claimed that –NCO adsorbed onto Ag–O–Al_{tetra} was activated, however, was stabilized on Ag–O–Al_{octa}.

The DOS diagrams depicted in Fig. 7 were consistent with the former results. Because changes in the C–O bond were minimal, we focused on the N–C bond. As shown in Fig. 7, the free –NCO anion has eight orbitals. The peak around –16 to –14.5 eV could be assigned to the N–C σ bond, whereas the peak around –4.5 to –3 eV could be ascribed to the N–C π bond. Upon adsorption onto the two types of Ag–O–Al entities, strong interactions between –NCO and Ag–O–Al_{tetra} were identified. The N–C σ bond close to Ag–O–Al_{tetra} displayed a "resonance" with the oxide metal surface and was delocalized via electron forward donation to an appropriate hybrid on a partner metal fragment, and back donation involving Ag and Al in the energy level of –5 to –3 eV to the π bond of N–C was observed. In the absence of Ag on Al_2O_3, –NCO could not be activated adequately, thereby indicating that interactions between Ag and Al are essential. Furthermore, in the absence of Ag species, back donation from the Ag d orbital to the N–C π bond did not occur. Comparison of the Ag^+ on the different Al sites showed that the

Ag–O–Al_{tetra} entity could activate adsorbates such as –NCO to a great extent. Thus Ag–O–Al_{tetra} rather than Ag–O–Al_{octa} entities are more plausible as the active sites during the HC-SCR process.

4. Conclusions

Ag^+ species anchored to Al_2O_3 (110) and (100) surfaces were examined to construct Ag/Al_2O_3 catalysts containing Ag–O–Al_{tetra} and Ag–O–Al_{octa} entities. Al_{trip} and $Al_{penta-a}$ sites on the (110) and (100) surfaces of Al_2O_3 were the respective precursors for the formation of these entities. Comparison of the two Ag–O–Al entities revealed that the Ag–O–Al_{tetra} entity could activate ethanol, and enolic and isocyanate species to a greater extent than the Ag–O–Al_{octa} entity. Therefore, the Ag–O–Al_{tetra} entity can more plausibly be regarded as the active site. Owing to the strong Lewis acidity of Al_{tetra}, the C–O bond in C_2H_5OH was activated via C–O σ bond forward donation to oxide metal sites. Key intermediates –NCO species were activated by elongation of the N–C bond. The N–C σ bond close to Ag–O–Al_{tetra} displayed a "resonance" with the metal oxide surface and in particular with the strong acid Al site, and was delocalized via electron forward donation. Electron back donation involving Ag and Al to the π bond of N–C was also observed. This finding

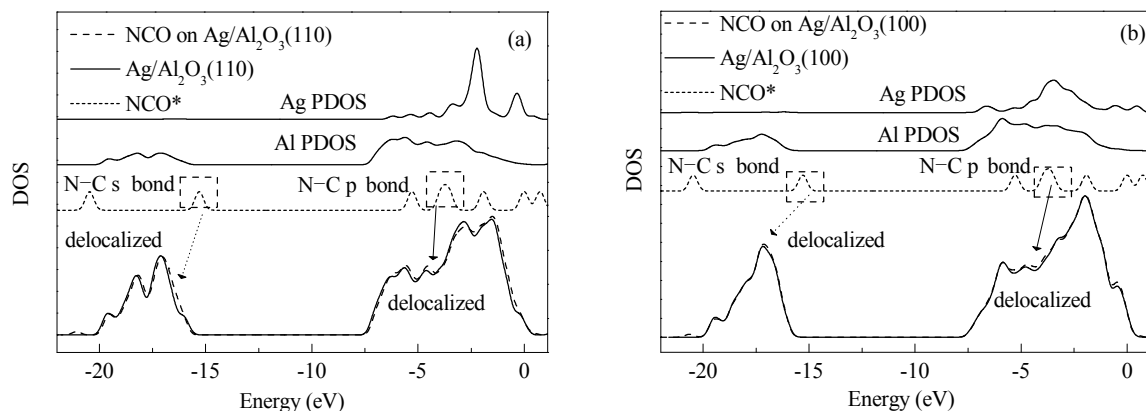**Fig. 7.** Total DOS and atom-resolved projected DOS (PDOS) analysis of –NCO adsorbed onto (a) Ag/Al_2O_3 (110) surface (Ag–O–Al_{tetra} entities) and (b) Ag/Al_2O_3 (100) surface (Ag–O–Al_{octa} entities).

Graphical Abstract

Adsorption states of typical intermediates on Ag/Al$_2$O$_3$ catalyst employed in the selective catalytic reduction of NO$_x$ by ethanol

Hua Deng, Yunbo Yu*, Hong He*

Research Center for Eco-Environmental Sciences, Chinese Academy of Sciences

Ag-O-Al$_{tetra}$ entities activated ethanol, and enolic and isocyanate species to a greater extent than Ag-O-Al$_{octa}$. The acidity of Al$_{tetra}$ and interaction between Ag and Al strongly influenced activation of −NCO via N−C bond elongation.
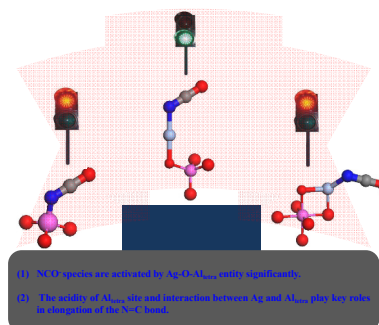
confirmed that the interaction between Ag and Al was essential in the HC-SCR process.

References

[1] Morin S, Savarino J, Frey M M, Yan N, Bekki S, Bottenheim J W, Martins J M F. *Science*, 2008, 322: 730

[2] He H, Ma Q X, Ma J Z, Zhang H X, Wang Y S, Ji D S, Tang G Q, Chu B W, Liu C, Hao J M. *Sci Rep*, 2014, 4: 4172

[3] Burch R, Breen J P, Meunier F C. *Appl Catal B*, 2002, 39: 283

[4] Shimizu K I, Satsuma A. *Phys Chem Chem Phys*, 2006, 8: 2677

[5] Liu Z M, Woo S I. *Catal Rev Sci Eng*, 2006, 48: 43

[6] He H, Zhang X L, Wu Q, Zhang C B, Yu Y B. *Catal Surv Asia*, 2008, 12: 38

[7] Granger P, Parvulescu V I. *Chem Rev*, 2011, 111: 3155

[8] Meunier F C, Ross J R H. *Appl Catal B*, 2000, 24: 23

[9] Bethke K A, Kung H H. *J Catal*, 1997, 172: 93

[10] He H, Zhang R D, Yu Y B, Liu J F. *Chin J Catal*, 2003, 24: 788

[11] Yu Y B, He H, Feng Q C. *J Phys Chem B*, 2003, 107: 13090

[12] She X, Flytzani-Stephanopoulos M. *J Catal*, 2006, 237: 79

[13] Zhang R D, Kaliaguine S. *Appl Catal B*, 2008, 78: 275

[14] Deng H, Yu Y B, Liu F D, Ma J Z, Zhang Y, He H. *ACS Catal*, 2014, 4: 2776

[15] Liu Z M, Ma L L, Junaid A S M. *J Phys Chem C*, 2010, 114: 4445

[16] Hu C H, Chizallet C, Mager-Maury C, Corral-Valerom M, Sautet P, Toulhoat H, Raybaud P. *J Catal*, 2010, 274: 99

[17] Digne M, Sautet P, Raybaud P, Euzen P, Toulhoat H. *J Catal*, 2002, 211: 1

[18] Digne M, Sautet P, Raybaud P, Euzen P, Toulhoat H. *J Catal*, 2004, 226: 54

[19] Lee J H, Yezerets A, Kung M C, Kung H H. *Chem Commun*, 2001: 404

[20] Yeom Y H, Li M J, Sachtler W M H, Weitz E. *J Catal*, 2006, 238: 100

[21] Tamm S, Ingelsten H H, Palmqvist A E C. *J Catal*, 2008, 255: 304

[22] Yu Y B, He H, Feng Q C, Gao H W, Yang X. *Appl Catal B*, 2004, 49: 159

[23] Yu Y B, Gao H W, He H. *Catal Today*, 2004, 93-95: 805

[24] He H, Yu Y B. *Catal Today*, 2005, 100: 37

[25] Satsuma A, Shimizu K I. *Prog Energy Combus Sci*, 2003, 29: 71

[26] Sumiya S, He H, Abe A, Takezawa N, Yoshida K. *J Chem Soc Faraday Trans*, 1998, 94: 2217

[27] Chansai S, Burch R, Hardacre C, Breen J, Meunier F. *J Catal*, 2010, 276: 49

[28] Chansai S, Burch R, Hardacre C, Breen J, Meunier F. *J Catal*, 2011, 281: 98

[29] Gao H W, He H. *Spectrochim Acta A*, 2005, 61: 1233

[30] Zhao S, Ren Y L, Wang J J, Yin W P. *J Mol Struct: THEOCHEM*, 2009, 897: 100

[31] He H, Li Y, Zhang X L, Yu Y B, Zhang C B. *Appl Catal A*, 2010, 375: 258

[32] Kim M K, Kim P S, Baik J H, Nam I S, Cho B K, Oh S H. *Appl Catal B*, 2011, 105: 1

[33] Breen J P, Burch R, Hardacre C, Hill C J. *J Phys Chem B*, 2005, 109: 4805

[34] Shimizu K I, Tsuzuki M, Kato K, Yokota S, Okumura K, Satsuma A. *J Phys Chem C*, 2007, 111: 950

[35] Korhonen S T, Beale A M, Newton M A, Weckhuysen B M. *J Phys Chem C*, 2011, 115: 885

[36] Yan Y, Yu Y B, He H, Zhao J J. *J Catal*, 2012, 293: 13

[37] Kwak J H, Hu J Z, Kim D H, Szanyi J S, Peden C H F. *J Catal*, 2007, 251: 189

[38] Kwak J H, Hu J Z, Lukaski A, Kim D H, Szanyi J S, Peden C H F. *J Phys Chem C*, 2008, 112: 9486

[39] Kwak J H, Mei D H, Yi C W, Kim D H, Peden C H F, Allard L F, Szanyi J. *J Catal*, 2009, 261: 17

[40] Kwak J H, Hu J Z, Mei D H, Yi C W, Kim D H, Peden C H F, Allard L F, Szanyi J. *Science*, 2009, 325: 1670

[41] Deng H, Yu Y B, He H. *J Phys Chem C*, 2015, 119: 3132

[42] Ukisu Y, Sato S, Muramatsu G, Yoshida K. *Catal Lett*, 1991, 11: 177

[43] Deng H, Yu Y B, He H. *Catal Today*, 2015, http://dx.doi.org/10.1016/j.cattod.2015.03.023

[44] Hoffman R. *Rev Mod Phys*, 1988, 60: 601

[45] Glassey W V, Hoffmann R. *Surf Sci*, 2001, 475: 47

Page numbers refer to the contents in the print version, which include both the English version and extended Chinese abstract of the paper. The online version only has the English version. The pages with the extended Chinese abstract are only available in the print version.